Published in final edited form as:
J Am Chem Soc. 2012 January 18; 134(2): 820–823. doi:10.1021/ja209650h.

Insights into the Mechanistic Dichotomy of the Protein Farnesyltransferase Peptide Substrates CVIM and CVLS

Yue Yang[†], **Bing Wang**[†], **Melek N. Ucisik**[†], **Guanglei Cui**[†], **Carol A. Fierke**[‡,*], and **Kenneth M. Merz Jr.**[†,*]

[†]Department of Chemistry and the Quantum Theory Project, 2328 New Physics Building, P.O. Box 118435, University of Florida, Gainesville, Florida, 32611-8435

[‡]Departments of Chemistry and Biological Chemistry, The University of Michigan, Ann Arbor, Michigan, 48109-1055

Abstract

Protein farnesyltransferase (FTase) catalyzes farnesylation of a variety of peptide substrates. ^{3}H α-secondary kinetic isotope effect measurements of two peptide substrates, CVIM and CVLS, are significantly different and have been proposed to reflect a rate-limiting S_N2-like transition state with dissociative characteristics for CVIM, while, due to the absence of an isotope effect, CVLS was proposed to have a rate-limiting peptide conformational change. Potential of mean force QM/MM studies coupled with umbrella sampling techniques were performed to further probe this mechanistic dichotomy. We observe the experimentally proposed TS for CVIM, but find that CVLS has a symmetric S_N2 TS, which is also consistent with the absence of a ^{3}H α-secondary kinetic isotope effect. These calculations demonstrate facile substrate- dependent alterations in the transition state structure catalyzed by FTase.

Keywords

FTase; farnesylation; zinc; mechanism; QM/MM; SCC-DFTB; PMF

Protein farnesyltransferase (FTase) and protein geranylgeranyltransferase type I (GGTase I) have been extensively studied, due to their involvement in cancer and potentially targets for cancer treatment[1]. Both enzymes catalyze the posttranslational attachment of a prenyl group (FTase: 15-carbon farnesyl, GGTase I: 20-carbon geranylgeranyl) to a cysteine residue in a conserved Ca_1a_2X sequence at or near the C-terminus of a protein (see Figure 1). C refers to cysteine, a_1 is an amino acid with little sequence selectivity, a_2 is an aliphatic amino acid, and X typically corresponds to alanine, serine, methionine (for FTase), phenylalanine (for FTase and GGTase I) or leucine (for GGTase I)[2]. This motif can be recognized and modified by FTase or GGTase I in the form of either a protein, like Ras, or a short peptide. Prenylation is essential to the function of a variety of enzymes including multiple Ras subfamily members, enabling them to localize to the cell membrane to play roles in signal regulation. Therefore, inhibition of prenylation could be used in the treatment of certain types of cancers by affecting the function of mutated Ras enzymes (found in about 30% of human cancers[3]). Indeed, several FTase inhibitors have entered Phase III clinical trial and have shown promise[4].

[*]**Corresponding Author** merz@qtp.ufl.edu; Tel: (352)392-6973; Fax: (352)392-8722.

ASSOCIATED CONTENT

Supporting Information. Methods and computation details, short trajectory movies and key structures. This material is available free of charge via the Internet at http://pubs.acs.org.

FTase and GGTase I possess very similar overall structures: they share nearly identical α-subunits and highly homologous β-subunits. The binding pocket for their respective reactants, Ca_1a_2X and the corresponding isoprenoid diphosphate, are situated at the interface of two subunits, surrounded by the conserved residues, Lys164α, His248β (His219β), Arg291β (Arg263β), Lys294β (Lys266β) and Tyr300β (Tyr272β) (Residues in parenthesis refer to those in GGTase I throughout). Both enzymes require a zinc ion for catalytic activity. In their activated forms, zinc is coordinated to Cys1p (targeted Ca_1a_2X cysteine), Asp297β (Asp269β), Cys299β (Cys271β) and His362β (His321β), forming a tetrahedral cluster. Fierke and coworkers determined that Cys1p is a thiolate rather than a thiol based on pH dependence studies[5]. In the crystal structures (1QBQ[6] and 1TN8[7] ~2Å resolution), the Zn^{2+}-$S_{Cys299\beta}$ distance is 0.1–0.2Å shorter than the Zn^{2+}-S_{Cys1p} distance, suggesting weaker coordination between the zinc and peptide cysteine. This weak coordination has been proposed to enhance the nucleophilicity of the sulfur atom of the target cysteine that is essential for the S_N2-like reaction[8]. In the crystal structure of FTase complexed with the prenylated K-Ras product (PDB code 1KZP[9], 2.10Å resolution), the Zn^{2+}-S_{Cys1p} distance increases to 2.66Å, providing additional support for this hypothesis[9]. FTase also requires a magnesium ion for optimal reactivity, but the position of this ion has not been observed crystallographically. Mutagenesis studies suggest that Asp352β coordinates magnesium[10,11]. Interestingly, in GGTase I, which is not activated by magnesium, this residue is a lysine (Lys311β) that has been proposed to functionally substitute for the Mg^{2+} ion[12]. Although farnesyl diphosphate (FPP) can exist as fully deprotonated form or its mono-protonated form (FPPH) at physiological pH in the absence of magnesium[5], previous computational work suggested the FPPH form, with one of the β-diphosphate oxygen atoms protonated, is preferred in this situation.[13]

An important feature of the ternary (FTase/FPP/Ca_1a_2X) resting state (RS) is a C_1-S_γ distance of over 7 Å. A conformational transition exclusively associated with FPP and the peptide substrate (not the enzyme) is required to close this gap prior the chemical step[9,10,13,14] (see Figure S1). The catalytic mechanism of the subsequent chemical step has been debated for a number of years. Evidence supporting both a S_N2-like mechanism (associative) and a S_N1-like mechanism (dissociative) have been put forward[15–17]. However, recent experimental and computational studies strongly support an associative mechanism with dissociative characteristics[18,19]. Additionally, research carried out in Fierke lab revealed that substrate recognition by FTase is context dependent[20], which illustrated that the identity of both X and a_2 play important roles in the catalytic efficiency. Moreover, in ^3H α-secondary kinetic isotope effect (α-SKIE) experiments, a value of near unity (1.00±0.04) was obtained for FTase catalyzing single turnover farnesylation of GCVLS while a significantly larger value (1.154±0.006) was observed for FTase with the peptide TKCVIF[19]. This difference was attributed to the presence of different rate-determining steps (RDS), which were proposed to involve the chemical step for FTase/TKCVIF, while for FTase/GCVLS the physical or conformational change step was hypothesized to be rate-limiting. This is an interesting observation given that the free energy of activation for farnesylation catalyzed by FTase is ~20 kcal/mol and the conformational change is localized to the substrates and not the enzyme (see Figure S1), which suggests that the peptide conformational transition is very highly constrained in FTase/GCVLS. Herein we describe studies testing this observation.

When we investigated the conformational transition step using potential of mean force (PMF) studies for the FTase/CVIM and FTase/CVLM complexes with classical molecular dynamics (MD) simulations, only small differences in the free energy barriers of the conformational step were observed[13]. This result indicated that a single change in the a_2 position of the Ca_1a_2X motif was unable to alter the RDS, but did not address the situation where both X and a_2 were altered in the Ca_1a_2X motif. Moreover, the details of the chemical

step following the conformational step were not studied. Hence, a QM/MM study was carried out in order to further elucidate both the conformational and chemical steps in FTase catalysis. In fact, although MD simulations carried out at the molecular mechanical (MM) level provided useful insights into the conformational step in FTase[13,21–23], theoretical studies at the QM/MM[24] level add an extra dimension.[18,25,26]. In particular, in the chemical step where bond breaking and forming are important, classical MM theory is inappropriate. The self-consistent-charge density-functional tight-binding (SCC-DFTB) method has become a popular choice in QM/MM simulations, especially in zinc metalloenzymes and those cases involving phosphate reactions[27–31]. Moreover, SCC-DFTB/MM method has been extensively tested and good accuracy has been reported[32–35]. Furthermore, a recent SCC-DFTB based computational study by Roitberg and coworkers elucidated the catalytic mechanism and successfully reproduced the experimental KIE in *trypanosoma cruzi transsialidase*[36]. Hence, SCC-DFTB was adopted to study the farnesylation reaction catalyzed by both FTase/FPPH/CVIM (CVIM) and FTase/FPPH/CVLS (CVLS) complexes.

The acetyl-capped CVIM peptide represents the Ca_1a_2X motif of human K-Ras, the mutant of which is usually found in lung cancers. After equilibration with the QM/MM potential, a steered MD (SMD) simulation was conducted to propagate the trajectory along the reaction coordinate (RC) defined as the distance between the two reacting atoms: the C_1 carbon from FPPH and the S_γ from the peptide cysteine. Including the C_1-O_1 bond into the RC results in an unphysical dissociative pathway and this same observation has been reported by Klein and coworkers[18] (see SI for further comparisons between this work and Ref 18). The RC ranged from 1.8 Å to 8.0 Å (6.2 Å in total) that covered both the conformational and chemical steps. The free energy curve yielded a C_1-S_γ distance of approximate 2.6 Å at the transition state (TS). This value is slightly longer than the 2.4–2.5Å TS C-S distance found in a model S_N2 reaction studied at the MP2/6-31+G**//MP2-6-31+G* level of theory[37]. Subsequently, a set of umbrella sampling simulations (US) were carried out along the RC and the WHAM code[38] was employed to construct the free energy profile. Our results indicate that farnesylation by FPPH, indeed, involves, an associative mechanism with dissociative character. The highest free energy barrier is 20.6 kcal/mol, and corresponds to the chemical step and is in excellent agreement with experimental results[16,19] (see Figure 2). Moreover, the conformational transition along the reaction coordinate matches our previous MM study, with a 6.9 Å (7.2 Å from MM) RS, 5.3 Å (5.0 Å from MM) intermediate and an ~1.0 kcal/mol energy barrier separating them[13]. Importantly, another shallow intermediate state was identified between the 5.3 Å intermediate and the TS at around 3.9 Å, where the O_1, C_1 and S_γ atoms are aligned in a linear arrangement which is favorable for S_N2 displacement. At the TS (see Figure 3), the H_1-H_2-C_1-C_2 dihedral is 169°, puckered slightly from a planar arrangement, moreover, the sign of this dihedral changes beyond this point, strengthening the point that the TS has been reached. The $d_{C1\text{-}S\gamma}$ distance is 2.63Å, the C_1-O_1 bond is breaking and reaches 2.3–2.5Å, while Zn-S_γ distance shows a 0.05Å increase, indicating a weaker coordination between zinc and peptide cysteine. Beyond the TS, the $d_{C1\text{-}S\gamma}$ continues decreasing, the $d_{C1\text{-}O1}$ distance keeps quickly increasing until around 3.5 Å, and the $d_{Zn\text{-}S\gamma}$ reaches 2.50–2.55Å in the product state. Throughout the entire reaction, key residues in the FPPH binding pocket, such as Lys164α, His248β, Arg291β, Lys294β and Tyr300β, all form stabilizing hydrogen bonds with the diphosphate-leaving group. The Zn(II) coordination site is maintained during the process, but the $d_{Zn\text{-}S\gamma}$ increases from ~2.35Å to ~2.50Å. Such an increase has also been discovered in the crystal structures reported by Long, *et al.*[9]. Additionally, Fierke and coworkers have proposed that a weak zinc-sulfur coordination enhances the nucleophilicity of Sγ[8]. Qualitatively, our observed increase of the $d_{Zn\text{-}S\gamma}$ distance supports the notion of the enhanced nucleophilicity at Sγ.

The acetyl-capped CVLS peptide has the same Ca_1a_2X sequence as H-Ras, whose malfunction has been implicated in bladder cancers. The PMF study was carried out on both

the physical step (at the MM level) and chemical step (at the QM/MM level). The free energy barrier associated with the conformational transition is ~2.8 kcal/mol. This value is of the same order of magnitude as observed for CVIM (~1.0 kcal/mol, at both QM/MM and MM level), FTase/FPPH/CVLM (~2.5 kcal/mol) and Yβ300F/FPPH/CVIM (~1.4 kcal/mol). Obviously, such a small barrier is insufficient to cause the predicted RDS change. In fact, the experimental free energy barrier height for FTase/GCVLS is 20 kcal/mol (in the absence of Mg^{2+}), while our QM/MM results gave a 21.3 kcal/mol free energy barrier, not for the physical step, but for the chemical step. Hence, another hypothesis needs to be developed to explain the observed near unity ^{3}H α-SKIE measurement. However, the possibility that an upstreaming sequence (TK) also influences α-SKIE cannot be excluded and is being explored.

α-SKIEs are useful in distinguishing S_N1 and S_N2 reaction types because they are sensitive to bond hybridization changes and the resultant changes in zero point energies (ZPEs). In a typical symmetrical S_N2 reaction, k_H/k_T tends to be smaller and near unity (~1.00±0.06), while the values observed for S_N1 reactions are ~1.1–1.2[39]. In the CVLS chemistry step, $d_{C1\text{-}S\gamma}$ at the TS is 2.51 Å (see Figure 3), which is 0.12 Å shorter than what was found for CVIM, and much closer to the value reported by Gronert *et al*. in their study of a related S_N2 reaction involving sulfur at the MP2/6-31+G**//MP2-6-31+G* level of theory[37]. At the TS, the O_1, C_1 of FPPH and S_γ of Cys1p are nearly co-linear with only C_1 being slightly out of plane and the C_1-O_1 bond is more constrained, reaching only 1.8–2.0Å and continues to slowly increase beyond the TS. The H_1-H_2-C_1-C_2 dihedral is nearly planar in the TS with a value of 179.6°, which decreases rapidly on both sides of this peak (see Figure S2). Hence, the structural evidence supports a more typical S_N2-like TS. During this reaction, the binding pocket amino acids do not experience large fluctuations, further confirming that an enzyme based conformational change that large enough to alter the RDS is unlikely. The Zn(II) coordination site is maintained during the process with the $d_{Zn\text{-}S\gamma}$ increasing by about 0.1Å.

As mentioned previously, the most important factor in the differences between k_H and k_T is the ZPE. In the light of this, we performed a QM optimization followed by frequency analysis with the M06-2X/6-31+G** level of theory[40,41], on the QM part of the system abstracted from the prenylation TSs for CVIM and CVLS, respectively. Subsequently, we calculated the $\Delta\Delta E_{ZPE}$ for both CVLS and CVIM, based on: $\Delta\Delta E_{ZPE}=\Delta E_{ZPE\ T}-\Delta E_{ZPE\ H}$, where $\Delta E_{ZPE}=E_{ZPE\ TS}-E_{ZPE\ GS}$ for both H and T. A ~0.12 kcal/mol difference of $\Delta\Delta E_{ZPE}$ was identified, with the CVIM complex possessing the larger $\Delta\Delta E_{ZPE}$ (0.15±0.02 kcal/mol) and the CVLS complex having a $\Delta\Delta E_{ZPE}$ near zero (0.01±0.01 kcal/mol). This strengthens our proposal that the CVLS peptide prefers a S_N2-like reaction pathway. Moreover, these results are qualitatively in accordance with the experimental trends (an approximate 0.085 kcal/mol $\Delta\Delta G$ for FTase/TKCVIF in the absence of Mg^{2+}, see SI). More importantly, it demonstrates that the slight differences observed in the reaction mechanisms reflect the experimentally observed k_H/k_T differences. We also qualitatively monitored charge variation through the reaction course of CVLS and CVIM prenylation using Mulliken charges. The summation of the charges on the C_1, C_2 and C_3 atoms (comprising an allyl like group) of the farnesyl group are of particular interest, because in a dissociative reaction pathway the developing partial positive charge would be delocalized across this allyl fragment, while in a pure S_N2 reaction less positive charge would be developed in the TS. For CVIM +0.032q is delocalized into the ally moiety, which is ten times smaller (+0.003*q*) in CVLS. This result strengthens our conclusion that the reaction mechanism for CVLS is a typical S_N2 reaction (synchronous A_ND_N) and an associative mechanism with dissociative characteristics (dissociative A_ND_N) for CVLM. Providing further support for our results is the agreement between the computed and experimental free energies of activation. The free energy barrier for the CVLS peptide was computed to be 21.3 kcal/mol, in excellent agreement with the

20.0 kcal/mol experimental value[16]. In addition, the computed free energy barrier difference between CVLS and CVIM is approximately 0.8 kcal/mol, which also is in agreement with the experimentally observed ~0.5 kcal/mol difference (although the experimental result is measured in the presence of Mg^{2+})[20].

The residues in the a_2 and X positions in the Ca_1a_2X motif have been shown to strongly affect substrate selection, with selection of the side chain at the a_2 position dependent on both hydrophicity and volume[20]. The different behavior of the a_2 residue between CVIM and CVLS was monitored via a modified Ramachandran plot. In this plot, we monitored the a_2 residue in terms of Ψ-Φ torsion angles throughout the chemical step (see Figure S3), for both complexes. In CVIM, the Ile3p remained in the α-region, while for CVLS Leu3p fluctuates in the transition region connecting the α- and β-regions. We propose that in the CVLS system the peptide sacrifices its conformational stability to facilitate bringing the two substrates together, while for CVIM the peptide remains in the α-region, so the energetic cost of the conformational step is mainly attributed to the rotation of FPPH. Preliminary results show that for CVLM, the Leu3p also remains in the α-region (see Figure S3). Therefore, it appears that the differential a_2 behavior observed in the CVLS and CVIM (/CVLM) complexes cannot be fully attributed to a single change at the a_2 position but to a double change at the a_2 and X positions, in support of the context- dependent substrate recognition hypothesis of Fierke and co-workers[20].

In conclusion, we have put forth an alternative proposal for FTase catalysis that involves differential S_N1/S_N2-like behaviors as a function of the peptide to be farnesylated. Thus, FTase activity appears to be fully governed by the chemical step with the conformational step only playing a modest role. Furthermore, the small energetic differences between the S_N1 and S_N2 transition states in the enzymes allow substrate dependent alteration in the transition state structure.

Supplementary Material

Refer to Web version on PubMed Central for supplementary material.

Acknowledgments

The authors thank Dr. Adrian E. Roitberg and Dr. Nicole A. Horenstein and Dr. June Pais for helpful discussions, and the NIH for financial support this project through grants (GM044974) to K.M.M and (GM040602) for C.A.F.. We also thank Dr. Qiang Cui for sharing phosphors parameters for SCC-DFTB.

Funding Sources

ABBREVIATIONS

FTase	protein farnesyltransferase
TS	transition state
RS	resting state
(S)KIE	(secondary) kinetic isotope effect
RDS	rate-determining step
PMF	potential of mean force
MD	molecular dynamics
QM/MM	quantum mechanical molecular mechanical

SCC-DFTB	self-consistent-charge density-functional tight-binding
RC	reaction coordinate
SMD	steered molecular dynamics
US	umbrella sampling

REFERENCES

1. Zhang FL, Casey PJ. Annu. Rev. Biochem. 1996; 65:241–269. [PubMed: 8811180]
2. Lamphear CL, Zverina EA, Hougland JL, Fierke CA. The Enzymes-Protein prenylation/Part A. 2011; 29:207–234.
3. Cox AD. Drugs. 2001; 61:723–732. [PubMed: 11398905]
4. Doll RJ, Kirschmeier P, Bishop WR. Curr. Opin. Drug Discovery Dev. 2004; 7:478–486.
5. Saderholm MJ, Hightower KE, Fierke CA. Biochemistry. 2000; 39:12398–12405. [PubMed: 11015220]
6. Strickland CL, Windsor WT, Syto R, Wang L, Bond R, Wu Z, Schwartz J, Le HV, Beese LS, Weber PC. Biochemistry. 1998; 37:16601–16611. [PubMed: 9843427]
7. Reid TS, Terry KL, Casey PJ, Beese LS. J. Mol. Biol. 2004; 343:417–433. [PubMed: 15451670]
8. Tobin DA, Pickett JS, Hartman HL, Fierke CA, Penner-Hahn JE. J. Am. Chem. Soc. 2003; 125:9962–9969. [PubMed: 12914459]
9. Long SB, Casey PJ, Beese LS. Nature. 2002; 419:645–650. [PubMed: 12374986]
10. Pickett JS, Bowers KE, Fierke CA. J. Biol. Chem. 2003; 278:51243–51250. [PubMed: 14532266]
11. Yang Y, Chakravorty DK, Merz KM. Biochemistry. 2010; 49:9658–9666. [PubMed: 20923173]
12. Hartman HL, Bowers KE, Fierke CA. J. Biol. Chem. 2004; 279:30546–30553. [PubMed: 15131129]
13. Cui G, Merz KM Jr. Biochemistry. 2007; 46:12375–12381. [PubMed: 17918965]
14. Long SB, Hancock PJ, Kral AM, Hellinga HW, Beese LS. Proc. Natl. Acad. Sci. U. S. A. 2001; 98:12948–12953. [PubMed: 11687658]
15. Dolence JM, Poulter CD. Proc. Natl. Acad. Sci. U. S. A. 1995; 92:5008–5011. [PubMed: 7761439]
16. Huang CC, Hightower KE, Fierke CA. Biochemistry. 2000; 39:2593–2602. [PubMed: 10704208]
17. Edelstein RL, Weller VA, Distefano MD, Tung JS. J. Org. Chem. 1998; 63:5298–5299.
18. Ho MH, Vivo MD, Peraro MD, Klein ML. J. Chem. Theory Comput. 2009; 5:1657–1666.
19. Pais JE, Bowers KE, Fierke CA. J. Am. Chem. Soc. 2006; 128:15086–15087. [PubMed: 17117849]
20. Hougland JL, Lamphear CL, Scott SA, Gibbs RA, Fierke CA. Biochemistry. 2009; 48:1691–1701. [PubMed: 19199818]
21. Cui G, Wang B, Merz KM Jr. Biochemistry. 2005; 44:16513. [PubMed: 16342942]
22. Cui G, Li X, Merz KM Jr. Biochemistry. 2006; 46:1303–1311. [PubMed: 17260959]
23. Sousa SF, Fernandes PA, Ramos MJ. Bioorg. Med. Chem. 2009; 17:3369–3378. [PubMed: 19369081]
24. Warshel A, Levitt M. J. Mol. Biol. 1976; 103:227–249. [PubMed: 985660]
25. Sousa SF, Fernandes PA, Ramos MJ. Chemistry-a European Journal. 2009; 15:4243–4247.
26. Sousa SF, Fernandes PA, Ramos MJ. Proteins-Structure Function and Bioinformatics. 2007; 66:205–218.
27. Elstner M, Porezag D, Jungnickel G, Elsner J, Haugk M, Frauenheim T, Suhai S, Seifert G. Physical Review B. 1998; 58:7260–7268.
28. Elstner M, Cui Q, Munih P, Kaxiras E, Frauenheim T, Karplus M. J. Comput. Chem. 2003; 24:565–581. [PubMed: 12632471]
29. Yang Y, Yu HB, York D, Elstner M, Cui Q. J. Chem. Theory Comput. 2008; 4:2067–2084. [PubMed: 19352441]

30. Moreira NH, Dolgonos G, Aradi B, da Rosa AL, Frauenheim T. J. Chem. Theory Comput. 2009; 5:605–614.
31. Elstner M, Gaus MGM, Cui QA. J. Chem. Theory Comput. 2011; 7:931–948.
32. Guo H, Guo HB, Rao N, Xu Q. J. Am. Chem. Soc. 2005; 127:3191–3197. [PubMed: 15740159]
33. Guo H, Xu D, Cui G. J. Am. Chem. Soc. 2007; 129:10814–10822. [PubMed: 17691780]
34. Xu DG, Guo H. J. Am. Chem. Soc. 2009; 131:9780–9788. [PubMed: 19552427]
35. Xu DG, Wu SS, Guo H. J. Am. Chem. Soc. 2010; 132:17986–17988. [PubMed: 21138257]
36. Pierdominici-Sottile G, Horenstein NA, Roitberg AE. Biochemistry. 2011; 50:10150–10158. [PubMed: 22007596]
37. Gronert S, Lee JM. J. Org. Chem. 1995; 60:6731–6736.
38. Grossfield A. 1.6d ed.
39. Purich, DL.; Allison, RD. Handbook of Biochemical Kinetics. San Diego, CA: Academic Press; 2000.
40. Truhlar DG, Zhao Y. Theor. Chem. Acc. 2008; 120:215–241.
41. Truhlar DG, Zhao Y. Acc. Chem. Res. 2008; 41:157–167. [PubMed: 18186612]

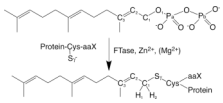

Figure 1.
FTase catalyzed farnesylation. Important atoms are labeled.

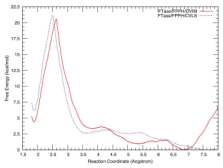

Figure 2.
Free energy profile of farnesylation catalyzed by FTase/FPPH/CVIM (red) and FTase/FPPH/CVLS (blue).

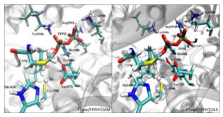

Figure 3.
TS active site snapshots of FTase/FPPH/CVIM (left) and FTase/FPPH/CVLS (right). Also see Figure S4.